Vibrational and Electronic Spectroscopy of Sulfuric Acid Vapor

Paul E. Hintze,[†] Henrik G. Kjaergaard,[‡] Veronica Vaida,*[,†] and James B. Burkholder[§]

Department of Chemistry and Biochemistry and Cooperative Institute for Research in Environmental Sciences, Campus Box 215, University of Colorado, Boulder, Colorado 80309, Aeronomy Laboratory, NOAA, 325 Broadway, Boulder, Colorado 80305-3328, and Department of Chemistry, University of Otago, P.O. Box 56, Dunedin, New Zealand

Received: June 22, 2002; In Final Form: October 27, 2002

We have measured and analyzed the infrared (IR), near-infrared (NIR) and vacuum ultraviolet (VUV) absorption spectra of vapor-phase sulfuric acid (H_2SO_4). Transitions associated with the fundamental vibrations and the first and second OH stretching overtones of this molecule have been identified. Our measured vibrational spectrum extends and complements those in the literature and agrees well with ab initio calculated spectra. We have calculated the fundamental and overtone OH stretching intensities with the use of a simple anharmonic oscillator local-mode model with ab initio calculated dipole-moment functions. Theory and experiment have been used to investigate the OH stretching vibrational overtones of H_2SO_4 and indicate that the OH stretching mode in H_2SO_4 is an important aspect of the spectroscopy of this atmospheric chromophore. We have attempted to measure the VUV spectrum of vapor-phase sulfuric acid and, in the absence of observed bands, give upper bounds to the photoabsorption cross section. We conclude that H_2SO_4 absorbs in the IR and NIR regions, with the OH stretching vibration playing the dominant role, and that the electronic excitation of H_2SO_4 will only be significant at very high energies, well above those available from the sun in the earth's atmosphere.

Introduction

The fundamental spectroscopic properties of vapor-phase sulfuric acid are required to evaluate the role of this atmospheric chromophore. The technical challenge of obtaining the spectra of this molecule is twofold: the vapor pressure of sulfuric acid is very low,[1] and spectra are complicated by the presence of SO_3 and H_2O, which are in equilibrium with H_2SO_4 and absorb radiation at similar energies. The low vapor pressure can be overcome by working at elevated temperatures, and subtraction of the reference spectra of SO_3 and H_2O can minimize the spectral interference.

Despite the importance of H_2SO_4 in the atmosphere, only a few experimental spectroscopic studies have been reported. The structure of H_2SO_4 was determined by microwave spectroscopy.[2] The studies in the IR region[3,4] have identified many of the fundamental transitions of H_2SO_4. For the SO_2 (S═O) symmetric stretching vibration alone, the integrated absorption coefficient has been reported.[5] The electronic excited states of H_2SO_4 vapor have been elusive. The only previous UV study did not detect any absorption that could be attributed to sulfuric acid and set an upper bound for the H_2SO_4 absorption cross section of 10^{-21} cm^2 molecule^{-1} in the 30 300−51 300 cm^{-1} range.[6]

In this paper, we present experimental and theoretical studies of H_2SO_4 vapor to complement and extend those available in the literature. We have measured the vibrational spectrum of vapor-phase sulfuric acid from 500 to 10 500 cm^{-1} and have assigned bands associated with fundamental stretching vibrations and the first and second OH stretching overtones. We have compared our recorded spectrum with results of ab initio calculated fundamental vibrational frequencies and intensities. We focused on developing an appropriate model for the OH stretching vibrations. Toward this end, we have calculated the OH stretching vibrational-band frequencies and intensities of H_2SO_4 with an anharmonic oscillator (AO) local-mode model. We used experimental local-mode parameters and ab initio calculated dipole-moment functions in our AO local-mode model.

The large-amplitude motion associated with XH stretching vibrations, where X is C, N, or O, has been well explained by the harmonically coupled anharmonic oscillator (HCAO) local-mode model.[7−10] CH stretching overtone intensities have been successfully predicted with the use of vibrational wave functions obtained with the HCAO local-mode model and ab initio calculated dipole-moment functions.[11−15] Kjaergaard and Henry previously found that accurate absolute overtone intensities can be obtained with the Hartree−Fock (HF) self-consistent-field method, provided a reasonably sized 6-311++G(2d,2p) basis set is used.[16] The hybrid density functional theory, B3LYP, and quadratic configuration interaction including singles and doubles (QCISD) theory improve the calculated intensities primarily in the fundamental region.[17,18] Here, we use ab initio calculations performed at the HF, B3LYP, and QCISD levels of theory with the 6-311++G(2d,2p) basis set. The calculated OH stretching frequencies and intensities are compared with experimental results and confirm that the local-mode model provides an appropriate description of the OH overtone vibrations of H_2SO_4.

To search for the elusive electronic spectrum of H_2SO_4, we have extended previous measurements[6] into the vacuum ultraviolet (VUV) region between 51 300 and 71 400 cm^{-1}. We have compared our measurements with calculations of the H_2SO_4 electronic transition energy[19] and found agreement in the conclusion that the electronic excitations in H_2SO_4 require very high energy.

* Corresponding author. E-mail: vaida@colorado.edu.
[†] University of Colorado.
[‡] On sabbatical at Cooperative Institute for Research in Environmental Sciences, University of Colorado.
[§] NOAA.

10.1021/jp0263626 CCC: $25.00
Published on Web 01/31/2003

Theory and Calculations

The geometry of H_2SO_4 was optimized at the HF, B3LYP, and QCISD levels of theory with the 6-311++G(2d,2p) basis set. The vibrational transition intensities of the fundamental normal modes were calculated with the B3LYP/6-311++G-(2d,2p) method and the harmonic-oscillator linear dipole-moment (HOLD) approximation within the Gaussian 94 suite of programs.[20] We have used a simple AO local-mode model[15] to describe the OH stretching vibrational modes in H_2SO_4. The coupling between the two OH stretching vibrations in H_2SO_4 will split the two OH stretching vibrations into symmetric and asymmetric vibrations. However, this coupling is small because of the significant spatial separation of the OH bonds. This splitting is not observed in our spectra; thus, we have neglected this coupling in our calculation of the OH stretching fundamental and overtone transitions within the AO local-mode model. The reported intensities are the sum of two OH stretches, which is the same as that seen in the experiment.

The AO local-mode model Hamiltonian for an isolated OH stretching oscillator can be written as[15]

$$(H - E_{|0\rangle})/hc = v\tilde{\omega} - (v^2 + v)\tilde{\omega}x \quad (1)$$

where $E_{|0\rangle}$ is the energy of the vibrational ground state and $\tilde{\omega}$ and $\tilde{\omega}x$ are the local-mode frequency and anharmonicity (in cm^{-1}) of the OH oscillator. The eigenstates of the AO Hamiltonian are taken as Morse-oscillator wave functions and are denoted by $|v\rangle$, where v is the vibrational quantum number. The local-mode parameters, $\tilde{\omega}$ and $\tilde{\omega}x$, can either be derived from a Birge−Sponer fit to the observed local-mode peak positions or calculated from an ab initio calculated potential-energy curve.[21] The Morse-oscillator frequency $\tilde{\omega}$ and anharmonicity $\tilde{\omega}x$ can be expressed in terms of the reduced mass of the oscillator and the second- and third-order ab initio calculated force constants F_{ii} and F_{iii} by[21]

$$\tilde{\omega} = \frac{\omega}{2\pi c} = \frac{(F_{ii}G_{ii})^{1/2}}{2\pi c} \quad (2)$$

$$\tilde{\omega}x = \frac{\omega x}{2\pi c} = \frac{hG_{ii}}{72\pi^2 c}\left(\frac{F_{iii}}{F_{ii}}\right)^2 \quad (3)$$

where G_{ii} is the reciprocal of the reduced mass. The force constants are obtained from a least-squares fit to an ab initio calculated one-dimensional potential-energy curve $V(q)$ as a function of the internal OH stretching displacement coordinate, q. We scale our ab initio calculated local-mode parameters to compensate for deficiencies in the ab initio method.[21] The scaling factors were determined as the ratio of calculated to experimental local-mode parameters of H_2O.[21,22] The uncertainty in $\tilde{\omega}x$ will lead to a small variation in the calculated intensities.

The oscillator strength f of a transition from the ground vibrational state $|0\rangle$ to a vibrationally excited state $|v\rangle$ is given by[14,23]

$$f_{v0} = 4.702 \times 10^{-7}[\text{cm D}^{-2}]\tilde{\nu}_{v0}|\vec{\mu}_{v0}|^2 \quad (4)$$

where $\tilde{\nu}_{v0}$ is the wavenumber of the transition and $\vec{\mu}_{v0} = \langle v|\vec{\mu}|0\rangle$ is the transition dipole-moment matrix element in debye (D). The calculated dimensionless oscillator strengths can be converted to units of km mol^{-1} by multiplication by 5.33×10^6 km mol^{-1}.[14] The vibrational wave functions are determined by the Hamiltonian eq 1, and we express the dipole-moment function as a series expansion in the OH displacement coordinate,[15,21]

$$\vec{\mu}(q) = \sum_i \vec{\mu}_i q^i \quad (5)$$

where $\vec{\mu}_i$ is $1/i!$ times the ith-order derivative of the dipole-moment function with respect to q. The coefficients $\vec{\mu}_i$ are obtained from a least-squares fit to an ab initio calculated one-dimensional dipole moment grid, $\vec{\mu}(q)$.

The one-dimensional grid is calculated by displacing the OH bond by ±0.2 Å from the equilibrium position in steps of 0.05 Å. At each grid point, the energy and dipole moment is calculated to provide both $V(q)$ and $\vec{\mu}(q)$. The dipole moments are calculated with the use of the generalized density for the specified level of theory, which will provide dipole moments that are the correct analytical derivatives of the energies. The nine-point grid with a step size of 0.05 Å provides good convergence of the dipole-moment derivatives and force constants. The choice of grid and step size is based on previous work.[21,24] The optimized geometries and all single-point calculations in the grids were calculated at a specified ab initio method with the use of Gaussian 94. The B3LYP optimizations and single-point calculations were run with an increased integration grid size (Keyword Int = 99434) to improve the convergence of the dipole derivatives.[25]

The excited electronic states of sulfuric acid were calculated with the Gaussian 98 suite of programs.[26] We have used the configuration interaction including singles (CIS) level of theory with the 6-311++G(d,p) basis set and the microwave-determined geometry.[2] Previously, a CIS/6-31G(d) calculation had been reported;[19] however, it has been shown that diffuse functions in the basis set are important in the CIS calculations of excited states.[27]

Experimental Section

The absorption spectrum of H_2SO_4 vapor was measured in the IR, near-infrared (NIR), and VUV regions with two separate instruments appropriate for the different energy regions studied. The temperature-controlled cells used for the two experiments were similar. The cell used in the IR/NIR regions had been used previously,[6] and the VUV cell was designed as a smaller version of this cell. Each cell had four inlet ports, two for the reactants and two for purging the windows, as well as a fifth exit port. The windows were attached using Viton O-ring seals. The condensation on the windows was checked by carefully monitoring the absolute light intensity on successive scans. The cells were wrapped with heating tape, insulation, and a layer of aluminum foil. The longer IR/NIR cell had a layer of copper foil between the glass and the heating tape. Thermocouple gauges were placed on the cell walls between the glass or copper foil and the heating tape to monitor the external temperature. The temperature of the gas inside the cell was measured by inserting a thermocouple into the cell while gases were flowing through at conditions similar to those used in the experiment.

Vapor-phase H_2SO_4 was generated in a 1:1 reaction of SO_3 and H_2O by titrating SO_3 with H_2O through a heated side arm of a temperature-controlled cell.[6] The amount of vapor-phase H_2SO_4 formed is a function of temperature. The temperature determined the vapor pressure of H_2SO_4. High temperatures of 130−150 °C were required to allow a measurable concentration of H_2SO_4 to be present. However, at temperatures above 150 °C the reaction shifts to the reactants, reducing the amount of H_2SO_4 present.

SO_3 was acquired by distillation from fuming sulfuric acid (~25% SO_3 in sulfuric acid). The IR spectrum of the distilled SO_3 showed no impurities of H_2O (<0.001 vol %) or SO_2 (<0.01 vol %). H_2O was doubly distilled. The samples were kept in glass containers that allowed the flow of the carrier gas to pass over the sample or bypass the sample completely. The carrier-gas flows were kept constant, even if one of the reactants was left out, to ensure that the temperature inside the cell was constant. The amount of SO_3 and H_2O introduced into the cell was controlled by keeping the sample in a controlled-temperature bath and could be varied so that different concentrations of H_2SO_4 could be generated.

IR and NIR Spectra. The vibrational spectra were collected using a Bruker 66IFS Fourier transform spectrometer (FTS). Light from the spectrometer was focused through the heated cell. The cell had a path length of 100 cm and an inner diameter of 5 cm, which tapered to 3 cm at the windows. The cell was heated to 150 °C. This temperature was found to produce the maximum amount of H_2SO_4 while producing no aerosols.

Spectra were recorded in the range of 500−10 500 cm^{-1} with a resolution of 1 cm^{-1} using three different experimental setups. The IR region was studied using a Globar IR source and DLATGS detector. The NIR region was studied using a tungsten lamp and either an InSb detector or InGaAs photodiode. Reference spectra of both SO_3 and H_2O were recorded with the same resolution and were subtracted from the H_2SO_4 spectra. Between 8 and 20 separate measurements were made with each detector. Each measurement had a different amount of H_2SO_4 present. Previously unassigned bands were related to the concentration of sulfuric acid by performing a linear regression on the integrated absorbances of the bands and that of the fundamental OH stretch. The bands that had a linear relationship are reported here as belonging to H_2SO_4.

The vibrational-band intensities of the observed transitions in H_2SO_4 were determined by integrating the area of the various bands. The band intensities are reported relative to that of the OH stretching transition with the use of a linear regression. The values reported in this work are the slopes of these regressions, and the reported uncertainties are 1 standard deviation of the slopes. Additional uncertainty will arise from the frequency limits defined for the integration of each band. This is especially important for overlapping bands. The frequency limits for the integration of overlapping bands were selected to occur at the point of minimum absorbance between the two bands. This will add uncertainty to the individual band intensities, although the combined intensities of overlapping bands should be very accurate.

One of the advantages of FTS is the wide spectral range that can be acquired during one scan. Because in FTS all frequencies are being measured simultaneously, the relative intensities that are determined should be accurate to better than 1%. The actual uncertainty reported is larger because of effects from overlapping bands.

VUV Spectra. Spectra in the VUV region were recorded with a 1-m Acton Research Corporation VUV monochromator. The slits on the monochromator had a width of 50 μm, which resulted in a resolution measured using a mercury lamp of 0.5 nm or 155 cm^{-1} at 60 000 cm^{-1}. The VUV cell had a path length of 10 cm and was made of a glass tube with an inner diameter of 2.5 cm. The windows were either Suprasil quartz or MgF_2. The temperature-controlled cell was placed in a vacuum compartment separated from the monochromator by a LiF window. The lamps used in our experiments were a Hamamatsu D_2 lamp (>170 nm) and Opthos Instruments Xe continuum lamp (155−180 nm) and Kr continuum lamp (140−170 nm). Two different photomultiplier tubes from Hamamatsu (R976 and R972) were used to cover the energy ranges studied. The pressure inside the cell was ~200 Torr and the temperature was 130 °C.

Spectral interference from SO_3 and H_2O was a considerable problem in the VUV region. Three separate measurements were recorded in series, bracketed by background spectra, to facilitate the subtraction of the SO_3 and H_2O reference spectra from the H_2SO_4 spectra. The first measurement was of pure SO_3. H_2O was then added to the flow, and the H_2SO_4 spectrum was recorded. The SO_3 flow was then shut off, and a pure H_2O spectrum was recorded.

The absorbance of a sample containing multiple absorbers is given by the sum of the absorbance of the individual samples. In the lower-energy spectrum recorded with the D_2 lamp, there was no detectable electronic absorption from H_2O at energies lower than 52 600 cm^{-1}. Thus, the amount of SO_3 in the H_2SO_4 spectra could be determined and an accurate SO_3 subtraction made. H_2O was then subtracted from the spectra. In the higher-energy spectra, recorded with the Xe and Kr lamps, there were no regions where either the SO_3 or the H_2O did not absorb. A mix of the SO_3 and H_2O reference spectra was fit to the H_2SO_4 spectra with a least-squares method. The residual spectrum was then considered to be the H_2SO_4 spectrum.

The concentration of H_2SO_4 was determined from the change in SO_3 concentration in the initial SO_3 scan and the H_2SO_4 scan and the 1:1 reaction of H_2O and SO_3 to form H_2SO_4. The SO_3 concentration is determined from the known cross sections[28] at 46 500 cm^{-1}. We used the H_2SO_4 concentration and the residual absorbance in the H_2SO_4 VUV spectra with the Beer−Lambert law to estimate an upper bound for the absorption cross section of H_2SO_4 in the measured range.

TABLE 1: Calculated and Observed Bond Lengths (in Å) of H_2SO_4

	calculated		
bond	B3LYP[a]	QCISD[a]	experimental[b]
OH	0.968	0.963	0.97
S═O	1.429	1.423	1.422
S−O	1.609	1.593	1.574

[a] Calculated with the 6-311++G(2d,2p) basis set. [b] From ref 2.

Results and Discussion

We have compared the ab initio calculated bond lengths for H_2SO_4 with experimental values determined from microwave spectroscopy[2] in Table 1. The agreement between the theoretical and experimental values is quite good and supports our choice of computational methods. In Figures 1S−6S (Supporting Information) we give the IR/NIR spectra of H_2SO_4 in the entire range from 500 to 10 500 cm^{-1} both before and after the subtraction of the H_2O and SO_3 reference spectra.

Fundamental Transitions. Selected regions of the IR spectrum of H_2SO_4 are shown in Figures 1 and 2. The experimental and calculated peak positions, assignments, and intensities are given in Table 2. The assignments and frequencies of the Q branch of the fundamental vibrational transitions are in good agreement with previous results.[3−5] The experimental and B3LYP/6-311++G(2d,2p) calculated relative intensities of most of the fundamental vibrations are within 36% of each other. When band overlap is taken into account, the agreement improves further, as will be discussed below. The agreement between the experimental and calculated relative intensities of the SOH bends and SO_2 symmetric stretching is not as good.

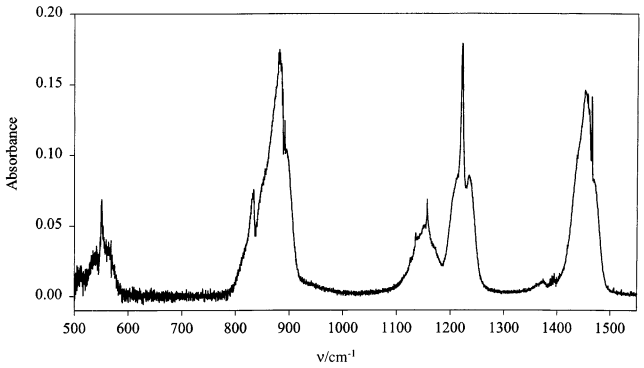

Figure 1. Vapor-phase IR spectrum of H_2SO_4 in the range of 500−1550 cm^{-1}. The spectrum was recorded at 150 °C with a path length of 100 cm. The reference spectra of H_2O and SO_3 have been subtracted.

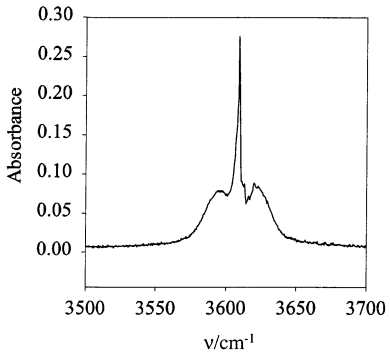

Figure 2. Vapor-phase IR spectrum of H_2SO_4 in the fundamental OH stretching region; $\Delta v_{OH} = 1$. The spectrum was recorded at 150 °C with a path length of 100 cm. The reference spectra of H_2O and SO_3 have been subtracted.

The frequencies of these three modes are calculated to be within 11 cm^{-1} of each other while the experimental frequencies are more than 60 cm^{-1} apart. This suggests that the modes are coupled and intensity is being shared between the three modes.

In the previous IR studies,[3,4] both the SO_2 bending and rocking modes were assigned. In our study, we were unable to find a clear feature to unambiguously assign the rocking mode. The position previously assigned to this mode (568 or 570 cm^{-1}) overlaps with the R branch of the bending mode. The reported intensity in Table 2 for the SO_2 bending mode might include the intensity for the rocking mode. If the calculated relative intensities of these two bands are added together, the sum (0.23) is close to the experimental value (0.26).

The S−O stretching modes are labeled $S(OH)_2$ stretch to be consistent with previous work. Our position for the Q branch of the $S(OH)_2$ asymmetric stretch is 8 cm^{-1} higher in energy than previously reported.[3,4] The assigned position in both of the previous studies appears to correspond to the point of maximum absorbance for this band. However, the higher resolution used in our study has allowed us to observe the Q branch at 891.4 cm^{-1} compared to the band maximum of 883 cm^{-1}. The P branch of this vibrational band has the largest intensity. The bands assigned to the $S(OH)_2$ symmetric (834.1 cm^{-1}) and asymmetric (891.4 cm^{-1}) stretches were resolved despite a large overlap. We have not deconvoluted the band, and thus the uncertainty in the intensity of each band will be higher than what is reported. However, the combined experimental intensity (2.01) is within 12% of the calculated intensity (1.77).

The band assigned to the SOH bend has several maxima. The intensity of the entire band scales linearly with the intensity of the OH stretch, so it is unlikely that an impurity is contributing to the absorbance of this band. In addition, none of the impurities likely to be present in the spectra (SO_3 or H_2O) have transitions in this energy region. We have chosen the highest peak at 1157.1 cm^{-1} as the Q branch for the asymmetric SOH bend in agreement with previous results.[3,4] The other features are left unassigned. The combined calculated relative intensity of the SOH bending modes is 80% greater than the experimental value. The calculation shows that there is strong mixing between the SOH bending modes and the SO_2 symmetric stretch, perhaps causing this discrepancy. The combined calculated intensities of the bending modes and the SO_2 symmetric stretch (1.3) is within 16% of the combined experimental value (1.54), suggesting that the three modes borrow intensity from each other.

The S═O stretching modes are labeled SO_2 stretch. The SO_2 asymmetric stretch, at 1464.7 cm^{-1}, is at higher energy compared to the previously assigned values of 1450 and 1456 cm^{-1}.[3,4] Similar to the $S(OH)_2$ asymmetric stretch, we resolve the Q branch of this band at our 1-cm^{-1} resolution whereas the previous studies seem to be of lower resolution.[3,4] We found

TABLE 2: Observed Transitions in the IR/NIR Vapor-Phase Spectra of H_2SO_4

	observed		literature		calculated[a]	
assignment	ν/cm^{-1}	rel intensity[b]	Chackalackal[c]	Stopperka[d]	ν/cm^{-1}	rel intensity
SO_2 bend	550.5	0.26 ± 0.09[e]	550	550	520	0.15
SO_2 rock			568	570	530	0.08
$S(OH)_2$ sym str	834.1	0.33 ± 0.01[f]	834	831	775	0.45
$S(OH)_2$ asym str	891.4	1.68 ± 0.06[f]	883	882	831	1.32
SOH sym bend			1138	1141	1174	0.63[g]
SOH asym bend	1157.1	0.54 ± 0.04[h,i]	1159	1160	1184	0.35[g]
SO_2 sym str	1220.1	1.00 ± 0.01[h]	1223	1224	1185	0.32[g]
SO_2 asym str	1464.7	1.34 ± 0.07	1450	1456	1437	1.18
SOH bend, $\Delta v_{SOH} = 2$	2278	1.9 (±0.2) × 10^{-2}				
SO_2 sym str + SO_2 asym str	2665	5.8 (±0.5) × 10^{-3}				
OH str, $\Delta v_{OH} = 1$	3609.2	1[j]	3610	3610	3769/3773	1[j]
	3820	1.9 (±0.1) × 10^{-2}				
OH str, $\Delta v_{OH} = 1$, + SOH bend	4739	1.2 (±0.1) × 10^{-2}				
OH str, $\Delta v_{OH} = 2$	7060.7	3.47 (±0.09) × 10^{-2}				
OH str, $\Delta v_{OH} = 2$, + SOH bend	8163	1.0 (±0.1) × 10^{-3}				
OH str, $\Delta v_{OH} = 3$	10 350.3	1.3 (±0.1) × 10^{-3}				

[a] Calculated with the B3LYP/6-311++G(2d,2p) method within the Gaussian 94 suite of programs. [b] The uncertainty is the standard deviation of the linear regression used to calculate the relative intensities. [c] Reference 3. [d] Reference 4. [e] This intensity may contain the intensity from the SO_2 rocking. [f] These bands overlap. [g] These bands are strongly coupled. [h] These bands overlap. [i] This intensity contains intensity from the symmetric bend. [j] Intensity set to 1.

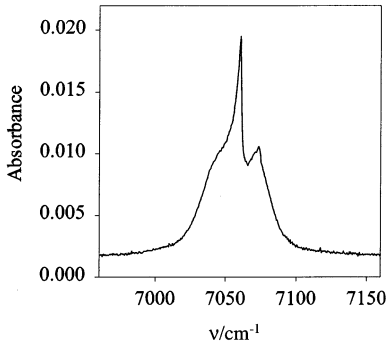

Figure 3. Vapor-phase NIR spectrum of H_2SO_4 in the first OH stretching overtone region, $\Delta v_{OH} = 2$. The spectrum was recorded at 150 °C with a path length of 100 cm. The reference spectrum of H_2O has been subtracted.

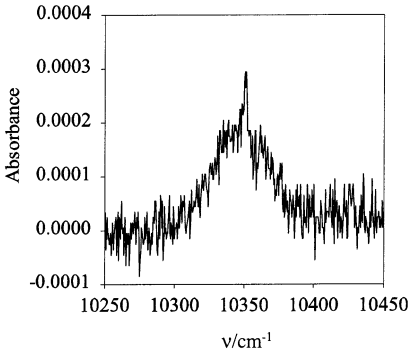

Figure 4. Vapor-phase NIR spectrum of H_2SO_4 in the second OH stretching overtone region, $\Delta v_{OH} = 3$. The spectrum was recorded at 150 °C with a path length of 100 cm.

the experimental intensity of both the symmetric and asymmetric SO_2 stretches to be somewhat higher than the calculated intensities. The SO_2 symmetric stretch observed at 1220.1 cm^{-1} was in good agreement with the previous values of 1222−1224 cm^{-1}.[3-5]

We have observed and assigned a few combination bands. The band at 2278 cm^{-1} is assigned to the first overtone or combinations of the SOH bend modes, and the band at 2665 cm^{-1} is assigned as the SO_2 symmetric and asymmetric stretches. We have assigned the bands at 3820 and 4739 cm^{-1} as combinations of the OH stretch with a low-energy torsional mode and the SOH bend, respectively.

Several of the bands, the $S(OH)_2$ asymmetric stretch and the OH stretch and its first overtone, show rotational structure. Studying the rotational structure of these vibrational bands is beyond the scope of the present work and would require higher resolution spectra.

The integrated absorption coefficient has previously been determined for the SO_2 symmetric stretch to be 460 ± 50 cm^{-2} atm^{-1} at 205 °C.[5] The integrated absorption coefficient can be converted to units of km mol^{-1} by multiplying it by 0.392.[29] This gives a value of 180 ± 20 km mol^{-1} for the SO_2 symmetric stretch. The absolute intensity of the bands reported here can be obtained from our accurate relative intensities and the literature value of the integrated absorption coefficient of the SO_2 symmetric stretch transition. Thus, the experimental intensity of the OH stretching band in H_2SO_4 is 180 ± 29 km mol^{-1} as we estimate an additional 5% uncertainty from the overlapping bands (SO_2 symmetric stretch).

OH Stretching Transitions. The measured OH stretching spectra of vapor-phase sulfuric acid corresponding to $\Delta v_{OH} = 1-3$ are shown in Figures 2−4.

The frequencies of the OH stretching transitions (3609.2, 7060.7, and 10 350.3 cm^{-1}) were fit to a Birge−Sponer equation obtained from eq 1 to determine the local-mode parameters given in Table 3. We have calculated the local-mode parameters with eqs 2 and 3. The experimental and calculated local-mode parameters are compared in Table 3. We see that the B3LYP/6-311++G(2d,2p) values, $\tilde{\omega} = 3771.2$ cm^{-1} and $\tilde{\omega}x = 82.7$ cm^{-1}, are quite good and would have predicted the OH stretching transitions in H_2SO_4 quite well. In fact, we used this calculated result to guide our search for the overtone transitions. The calculated local-mode frequencies vary by about 20 cm^{-1}, which would give rise to some uncertainty in the calculated peak positions of higher overtones. Kjaergaard has recently found a similar result for nitric acid[30] and concludes that the use of the scaling factors found for H_2O is less suitable for inorganic acids. The local-mode anharmonicities calculated with the three methods are quite similar and about 2−3 cm^{-1} higher than the experimentally determined value.

TABLE 3: Calculated and Observed OH Stretching Local-Mode Parameters in H_2SO_4

	calculated[a]			
	HF	B3LYP	QCISD	observed[b]
$\tilde{\omega}$/cm^{-1}	3793.0	3771.2	3790.0	3768.2 ± 1.3
$\tilde{\omega}x$/cm^{-1}	82.3	82.7	81.7	79.5 ± 0.4

[a] Scaling factors for $\tilde{\omega}$ and $\tilde{\omega}x$ respectively are 0.9210 and 0.897 for HF, 0.9985 and 0.872 for B3LYP, and 0.9836 and 0.850 for QCISD. [b] Determined from a Birge−Sponer fit to the observed transitions $\Delta v_{OH} = 1-3$. The uncertainty given is 1 standard deviation.

TABLE 4: Calculated and Observed Relative Intensities of OH Stretching Transitions in H_2SO_4

	observed		calculated[a]		
v	ν/cm^{-1}	rel intensity	ν/cm^{-1}	rel intensity[b]	rel intensity[c]
1	3609.2	1.0	3609.2	1.0	1.0
2	7060.7	3.5×10^{-2}	7059.4	3.4×10^{-2}	3.4×10^{-2}
3	10 350.3	1.3×10^{-3}	10 350.6	1.4×10^{-3}	1.0×10^{-3}

[a] Calculated with the experimental local-mode parameters from Table 3. [b] Calculated with the B3LYP/6-311++G(2d,2p) dipole-moment function. [c] Calculated with the QCISD/6-311++G(2d,2p) dipole-moment function.

The bond dissociation energy can be estimated from the local-mode parameters with the following equation, $D_e \approx \tilde{\omega}^2/4\tilde{\omega}x$. Using the experimental local-mode parameters in Table 3, a value of 46 400 cm^{-1}, or 133 kcal mol^{-1}, is obtained for the bond-dissociation energy. This is reasonably close to the value for a typical OH bond and supports our use of this model even though the local-mode parameters were obtained from only three experimental points.

We have calculated the frequencies and intensities of the OH stretching transition in H_2SO_4 with all three theoretical methods. In Table 4, we compare the observed and calculated relative OH stretching intensities. It has been shown that electron correlation is required to accurately predict the intensity of the fundamental transitions,[17,18] and thus only B3LYP and QCISD results are compared in Table 4. The agreement between both the calculations and the observed relative intensities is very good for $\Delta v_{OH} = 2$ and quite good for $\Delta v_{OH} = 3$. The B3LYP intensity is somewhat higher and the QCISD intensity somewhat lower than the observed intensity for $\Delta v_{OH} = 3$. The calculated transition frequencies for $\Delta v_{OH} = 1-3$ are in excellent agreement with the observed frequencies, as is expected from the low uncertainty on the experimentally determined local-mode parameters. This suggests that the Morse potential is a good model for at least the $v = 1-3$ energy levels. In a previous

TABLE 5: Calculated OH Stretching Oscillator Strengths in H_2SO_4

v	ν^a/cm^{-1}	HF	B3LYP	QCISD
1	3 609.2	6.62×10^{-5}	3.86×10^{-5}	3.94×10^{-5}
2	7 059.4	9.89×10^{-7}	1.33×10^{-6}	1.33×10^{-6}
3	10 350.6	3.50×10^{-8}	5.34×10^{-8}	4.07×10^{-8}
4	13 482.8	2.09×10^{-9}	2.81×10^{-9}	2.28×10^{-9}
5	16 456.0	2.04×10^{-10}	2.13×10^{-10}	2.18×10^{-10}

[a] Calculated with the experimental local-mode parameters from Table 3. Oscillator strengths given are for the two OH bonds in H_2SO_4.

study of HNO_3, Kjaergaard found the Morse-potential energy levels to give good transition energies up to $\Delta v_{OH} = 5$.[30]

The experimental intensity of the fundamental OH stretching band was determined to be 180 km mol^{-1}. We have calculated the intensity of this band both with the HOLD approximation within Gaussian 94 and with the AO local-mode model. The HOLD-calculated combined intensity of the symmetric and asymmetric OH stretches is 252 km mol^{-1} with the B3LYP/6-311++G(2d,2p) method. The values obtained with the AO local-mode model are given in Table 5. With the B3LYP/6-311++G(2d,2p) method we get 205 km mol^{-1}, which is in good agreement with the experimental value and significantly better than the HOLD-calculated value. This suggests that the anharmonic potential and nonlinearity of the potential is important even for the fundamental OH stretching transition in H_2SO_4. With the QCISD/6-311++G(2d,2p) method, a value of 210 km mol^{-1} is obtained also in good agreement with the experimental value. The HF calculation overestimates the intensity (353 km mol^{-1}) as expected.[17]

In Table 5, we show a comparison of the absolute intensities calculated with the HF, B3LYP, and QCISD theories and the 6-311++G(2d,2p) basis set. The results are fairly similar between the three methods for the higher overtones and indicate the need for electron correlation for the fundamental and lower overtones.[17] The calculated intensities show the usual drop-off with increasing v.

On the basis of these results, we expect to be able to predict the frequency and absolute intensity of the higher overtones, which are too weak to be measured experimentally, with the AO local-mode model and a B3LYP/6-311++G(2d,2p) calculated dipole-moment function.

Both theory and experiment suggest that the OH stretching vibrations couple weakly to each other and to the other vibrational modes. This is evident by the small number of combination bands and the rapid decrease of the intensity of these combination bands with increasing overtone. These results point to the importance of the OH stretch as the active mode in the spectra of H_2SO_4. The lack of any local-mode combination bands is a good indication of the very small coupling between the two OH bands in H_2SO_4. In 1,3-butadiene, local-mode combination bands are observed even at $\Delta v_{OH} = 4$.[15]

Electronic Transitions. We have obtained VUV spectra with number densities of H_2SO_4 that range from 4×10^{14} to 3×10^{15} cm^{-3}. After the SO_3 and H_2O reference spectra were subtracted, the residual absorbance was found to be within the noise levels of the measurements. Thus, no absorbance bands could be attributed to H_2SO_4. We have estimated the upper bounds for the absorption cross section of 10^{-19} cm^2 molecule^{-1} in the 51 300−58 800 cm^{-1} range and of 10^{-18} cm^2 molecule^{-1} in the 58 800−71 400 cm^{-1} range. In the lower energy range 30 300−51 300 cm^{-1}, where little to no interference from SO_3 and H_2O exists, the upper bound for the absorption cross section has been reported to be 10^{-21} cm^2 molecule^{-1}.[6]

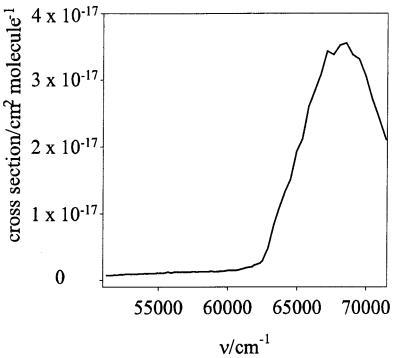

Figure 5. Vapor-phase VUV spectrum of SO_3. The spectrum was recorded at 130 °C with a path length of 10 cm.

The VUV reference spectrum of SO_3 in the 51 300−71 400 cm^{-1} range is shown in Figure 5. We determined the SO_3 concentration from the published cross sections[28] at 46 500 cm^{-1}. This SO_3 electronic band has a maximum cross section of $3.6 \pm 0.8 \times 10^{-17}$ cm^2 molecule^{-1} at 68 500 cm^{-1}. Cross sections from 51 300 to 71 400 cm^{-1} are reported in Table 1S (Supporting Information). We estimate the integrated absorption cross section of the band by integrating half the band and multiplying by 2 to be 3×10^{-17} cm molecule^{-1} or an oscillator strength of 0.3. In a previous study, the maximum cross section of this band was reported to be 2.6×10^{-17} cm^2 molecule^{-1}; however, their band had strong interference from SO_2 absorption.[31] We do not observe any signs of SO_2 in our spectra.

We have calculated the electronically excited states of SO_3 with the CIS/6-311+G(d) method. The first two electronically excited states of SO_3 with nonzero oscillator strengths both occur around 66 300 cm^{-1}, which is within 4% of our observed band maximum. The combined oscillator strength of these two transitions is calculated to be 0.07 compared to our experimental value of 0.3. The good agreement between the experimental and calculated transition energies for SO_3 supports the use of this theoretical method for the calculation of the transition energies of H_2SO_4.

Previously, the excited electronic states of H_2SO_4 were calculated with the CIS/6-31G(d) method.[19] This study found the first electronic transition with nonzero oscillator strength to occur at 90 200 cm^{-1}. It is known that the addition of diffuse functions in the basis set improves the CIS calculations of electronic excited states.[27] Thus, we have calculated the electronic excited states of H_2SO_4 with the CIS/6-311++G-(d,p) method. We found the first excited state to occur at 81 800 cm^{-1} with an oscillator strength of 0.018. Although this energy is somewhat lower than the previously calculated energy, it is significantly higher than the upper range of our experiment. Thus, our calculation supports the conclusion that there is no major electronic absorbance for H_2SO_4 at energies lower than 71 400 cm^{-1} and it is unlikely that any of the H_2SO_4 electronic transitions will extend into the range of our experiment.

Conclusions

We have employed a combined experimental and theoretical approach to investigate the vibrational and electronic spectroscopy of H_2SO_4 vapor. In this context, we have reported the experimental and theoretical frequencies and intensities for the fundamental and OH stretching overtone vibrational spectra of gas-phase sulfuric acid. The observed frequencies and relative intensities of the fundamental vibrational modes agree well with those obtained from a HOLD calculation with the B3LYP/6-311++G(2d,2p) method. We have used an AO local-mode

model with ab initio calculated dipole-moment functions to calculate the frequencies and intensities of the fundamental and overtone OH stretching transitions. The B3LYP/6-311++G-(2d,2p) calculations agree well with our observed frequencies and relative intensities for the observed $\Delta\nu_{OH} = 1-3$ transitions. The experimentally determined local-mode parameters fit well to a Morse-oscillator energy expression. The fundamental intensity determined with the B3LYP/6-311++G(2d,2p) method and the AO local-mode model agree better with the experimental value than does that of the HOLD mode calculation. These results lead us to believe that our AO local-mode model can be used to predict frequencies and intensities of higher vibrational overtones not amenable to observation.

The spectroscopic results presented here suggest that the OH stretch is the active mode in the NIR, visible, and ultraviolet spectra of the H_2SO_4 vapor. The electronic transitions of this molecule are not expected at energies below 71 400 cm^{-1} and, consequently, cannot be excited with solar photons in the earth's atmosphere.

Acknowledgment. P.E.H. would like to thank CIRES for a graduate fellowship. H.G.K. is grateful to CIRES for a visiting faculty fellowship. The National Science Foundation, the Marsden Fund administrated by the Royal Society of New Zealand, and the University of Otago have provided funding for this research.

Supporting Information Available: One table of SO_3 absorption cross sections from 51 300 to 71 400 cm^{-1}. Six figures with the IR/NIR spectra of H_2SO_4 in the range of 500−10 500 cm^{-1}. Two figures with the VUV spectra of H_2SO_4 in the range of 51 300−71 400 cm^{-1}. Spectra are shown both before and after the subtraction of the H_2O and SO_3 reference spectra. This material is available free of charge via the Internet at http://pubs.acs.org.

References and Notes

(1) Ayers, G. P.; Gillett, R. W.; Gras, J. L. *Geophys. Res. Lett.* **1980**, *7*, 433.
(2) Kuczkowski, R. L.; Suenram, R. D.; Lovas, F. J. *J. Am. Chem. Soc.* **1981**, *103*, 2561.
(3) Chackalackal, S. M.; Stafford, F. E. *J. Am. Chem. Soc.* **1966**, *88*, 723.
(4) Stopperka, K.; Kilz, F. *Z. Anorg. Allg. Chem.* **1969**, *370*, 49.
(5) Majkowski, R. F.; Blint, R. J.; Hill, J. C. *Appl. Opt.* **1978**, *17*, 975.
(6) Burkholder, J. B.; Mills, M.; McKeen, S. *Geophys. Res. Lett.* **2000**, *27*, 2493.
(7) Henry, B. R. *Acc. Chem. Res.* **1977**, *10*, 207.
(8) Mortensen, O. S.; Henry, B. R.; Mohammadi, M. A. *J. Chem. Phys.* **1981**, *75*, 4800.
(9) Child, M. S.; Lawton, R. T. *Faraday Discuss.* **1981**, 273.
(10) Sage, M. L.; Jortner, J. *Adv. Chem. Phys.* **1981**, *47*, 293.
(11) Mortensen, O. S.; Ahmed, M. K.; Henry, B. R.; Tarr, A. W. *J. Chem. Phys.* **1985**, *82*, 3903.
(12) Findsen, L. A.; Fang, H. L.; Swofford, R. L.; Birge, R. R. *J. Chem. Phys.* **1986**, *84*, 16.
(13) Tarr, A. W.; Zerbetto, F. *Chem. Phys. Lett.* **1989**, *154*, 273.
(14) Kjaergaard, H. G.; Yu, H. T.; Schattka, B. J.; Henry, B. R.; Tarr, A. W. *J. Chem. Phys.* **1990**, *93*, 6239.
(15) Kjaergaard, H. G.; Turnbull, D. M.; Henry, B. R. *J. Chem. Phys.* **1993**, *99*, 9438.
(16) Kjaergaard, H. G.; Henry, B. R. *Mol. Phys.* **1994**, *83*, 1099.
(17) Kjaergaard, H. G.; Daub, C. D.; Henry, B. R. *Mol. Phys.* **1997**, *90*, 201.
(18) Kjaergaard, H. G.; Bezar, K. J.; Brooking, K. A. *Mol. Phys.* **1999**, *96*, 1125.
(19) Wrenn, S. J.; Butler, L. J.; Rowland, G. A.; Knox, C. J. H.; Phillips, L. F. *J. Photochem. Photobiol., A* **1999**, *129*, 101.
(20) Frisch, M. J.; Trucks, G. W.; Schlegel, H. B.; Gill, P. M. W.; Johnson, B. G.; Robb, M. A.; Cheeseman, J. R.; Keith, T.; Petersson, G. A.; Montgomery, J. A.; Raghavachari, K.; Al-Laham, M. A.; Zakrzewski, V. G.; Ortiz, J. V.; Foresman, J. B.; Cioslowski, J.; Stefanov, B. B.; Nanayakkara, A.; Challacombe, M.; Peng, C. Y.; Ayala, P. Y.; Chen, W.; Wong, M. W.; Andres, J. L.; Replogle, E. S.; Gomperts, R.; Martin, R. L.; Fox, D. J.; Binkley, J. S.; Defrees, D. J.; Baker, J.; Stewart, J. P.; Head-Gordon, M.; Gonzalez, C.; Pople, J. A. *Gaussian 94*, Revision D.4; Gaussian, Inc.: Pittsburgh, PA, 1995.
(21) Low, G. R.; Kjaergaard, H. G. *J. Chem. Phys.* **1999**, *110*, 9104.
(22) Kjaergaard, H. G.; Henry, B. R.; Wei, H.; Lefebvre, S.; Carrington, T.; Mortensen, O. S.; Sage, M. L. *J. Chem. Phys.* **1994**, *100*, 6228.
(23) Atkins, P. W. *Molecular Quantum Mechanics*, 2nd ed.; Oxford University Press: New York, 1983.
(24) Kjaergaard, H. G.; Henry, B. R. *J. Chem. Phys.* **1992**, *96*, 4841.
(25) Kjaergaard, H. G.; Robinson, T. W.; Brooking, K. A. *J. Phys. Chem. A* **2000**, *104*, 11297.
(26) Frisch, M. J.; Trucks, G. W.; Schlegel, H. B.; Scuseria, G. E.; Robb, M. A.; Cheeseman, J. R.; Zakrzewski, V. G.; Montgomery, J. A., Jr.; Stratmann, R. E.; Burant, J. C.; Dapprich, S.; Millam, J. M.; Daniels, A. D.; Kudin, K. N.; Strain, M. C.; Farkas, O.; Tomasi, J.; Barone, V.; Cossi, M.; Cammi, R.; Mennucci, B.; Pomelli, C.; Adamo, C.; Clifford, S.; Ochterski, J.; Petersson, G. A.; Ayala, P. Y.; Cui, Q.; Morokuma, K.; Malick, D. K.; Rabuck, A. D.; Raghavachari, K.; Foresman, J. B.; Cioslowski, J.; Ortiz, J. V.; Stefanov, B. B.; Liu, G.; Liashenko, A.; Piskorz, P.; Komaromi, I.; Gomperts, R.; Martin, R. L.; Fox, D. J.; Keith, T.; Al-Laham, M. A.; Peng, C. Y.; Nanayakkara, A.; Gonzalez, C.; Challacombe, M.; Gill, P. M. W.; Johnson, B. G.; Chen, W.; Wong, M. W.; Andres, J. L.; Head-Gordon, M.; Replogle, E. S.; Pople, J. A. *Gaussian 98*, Revision A.6; Gaussian, Inc.: Pittsburgh, PA, 1998.
(27) Foresman, J. B.; Headgordon, M.; Pople, J. A.; Frisch, M. J. *J. Phys. Chem.* **1992**, *96*, 135.
(28) Burkholder, J. B.; McKeen, S. *Geophys. Res. Lett.* **1997**, *24*, 3201.
(29) Pugh, L. A.; Rao, K. N. *Mol. Spectrosc.: Mod. Res.* **1976**, *2*, 165.
(30) Kjaergaard, H. G. *J. Phys. Chem. A* **2002**, *106*, 2979.
(31) Suto, M.; Ye, C.; Ram, R. S.; Lee, L. C. *J. Phys. Chem.* **1987**, *91*, 3262.